31st Annual International Conference of the IEEE EMBS
Minneapolis, Minnesota, USA, September 2-6, 2009

Noninvasive deadbeat control of an implantable rotary blood pump: A simulation study

E. Lim, A. H. Alomari, A. V. Savkin and N. H. Lovell

Abstract— **A deadbeat controller has been proposed for the control of pulsatile pump flow in an implantable rotary blood pump (IRBP). A lumped parameter model of the cardiovascular system, in combination with the stable dynamical models of pulsatile flow and differential pressure (head) estimation for the IRBP was used to evaluate the controller. Pump speed and current were used as the only measured variables of the control system. The control algorithm was tested using both constant and sinusoidal reference pump flow input, under healthy and heart failure conditions. Results showed that the controller is able to track the reference input with minimal error in the presence of model uncertainty.**

I. INTRODUCTION

Congestive heart failure (CHF) is characterized by the inability of the heart to supply adequate blood flow and therefore oxygen delivery to tissues and organs in the body. The limitations of donor organ availability has led to a range of treatment alternatives for CHF patients, including implantable rotary blood pumps (IRBPs).

Due to the risk of thrombus formation associated with the implantation of flow or pressure sensors in the body, as well as their measurement drift with time, one design goal of an IRBP is to control the pump without the need for additional implantable sensors. Wu et al. [1] based their algorithms on the control of aortic pressure, which was estimated using a state-space model of the human circulatory system as well as measurements of pump differential pressure. On the other hand, Choi et al. [2] developed a fuzzy logic controller for an axial blood pump based on the blood flow pulsatility, estimated using a validated pump model. A limitation of the previous work was that the estimation of either pump flow or differential pressure was based on steady state pump modelling, which had not been validated during transient changes.

Furthermore, to date, pulsatile flow control of an IRBP has not been widely studied, despite potential concerns regarding their non-physiological hemodynamics which may cause alterations in biochemical function [3]. A few papers which looked into this included Korakianitis et al. [4] who performed computer simulations to study the effect of counter pulsation flow control on the hemodynamic response and Vandenberghe et al. [5] who studied the effect of various pulsatile mode support strategies on pressures and flows in a mock loop. However, we are not aware of any studies which evaluate the controller performance (operating in pulsatile mode) during transient changes of reference input or model parameters and under various simulated heart conditions.

The present paper uses a software model of the cardiovascular system (CVS) and an IRBP to evaluate the performance of a deadbeat controller in controlling pump flow of an IRBP noninvasively in both continuous and pulsatile modes.

E. Lim and N. H. Lovell are with the Graduate School of Biomedical Engineering, The University of New South Wales, Sydney, NSW, 2052, Australia (phone: +61 (2) 9385 5866; fax: +61 (2) 9385 3922. einly@student.unsw.edu.au; n.lovell@unsw.edu.au)

A. H. Alomari and A. V. Savkin are with the School of Electrical Engineering and Telecommunications, The University of New South Wales, Sydney, NSW, 2052, Australia (a.alomari@student.unsw.edu.au; a.savkin@unsw.edu.au)

This work was supported in part by the Australian Research Council.

II. MATERIALS AND METHODS

A. Model of the ventricular assisted circulatory system

A computer model consisting of a lumped-parameter model of the CVS and a stable dynamical model of left ventricular assist device (LVAD) was used to evaluate the control strategy. An electrical equivalent circuit analogue of the heart-pump interaction model is illustrated in Fig. 1. The model of the CVS consists of the left and right sides of the heart, as well as the pulmonary and systemic circulations. Each compartment in the CVS model was formulated based on well established experimental observations [7]. A detailed description of the model as well as parameter values, previously developed by our research group, can be obtained from [6]. The model has been carefully validated using published data from the literature, as well as our animal experiments using healthy pigs implanted with an LVAD. Model parameters associated with left ventricular failure (LVF), including contractility of the left ventricle, systemic vascular resistance, total blood volume and heart rate were then modified to allow simulations of moderate and severe LVF conditions. These parameters were carefully chosen in order to ensure that realistic simulation, in terms of cardiac output, aortic pressure and left atrial pressure, was achieved [8].

The LVAD model included the description of the rotary blood pump, as well as the inlet and outlet cannulae. Descriptions of the inlet and outlet cannulae can be found in [6]. Stable dynamical models for pulsatile flow and differential pressure estimation of the IRBP using non-invasive measurements of pump power, P, and rotational speed, ω, previously designed and verified using in vivo pig data and in vitro mock loop experimental data by our research group, were used in the present simulation to represent the pump model. Detailed descriptions of the models, including the system identification and validation methods used to obtain them can be found in [9].

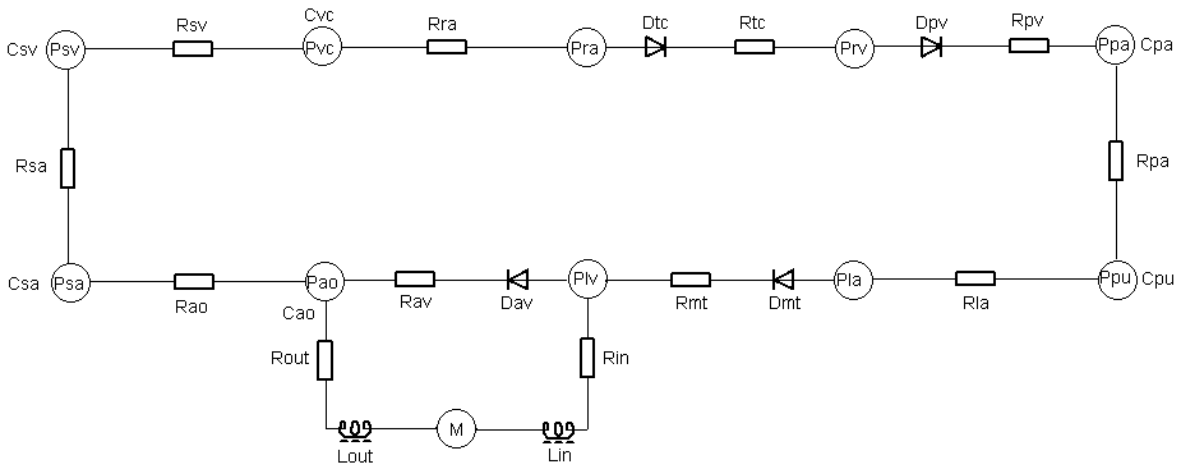

Fig. 1. Schematic diagram of the ventricular assisted circulatory system model. The capacitive elements (C_i) represent the compliance of the various compartments, while the resistive elements (R_i) represent the resistances between two compartments. For a description of each compartment see [6].

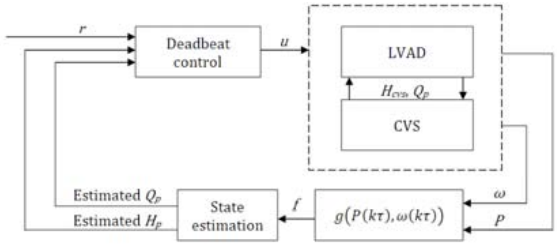

Fig. 2. Block diagram of the deadbeat control system.

The combined CVS - LVAD model was validated against experimental data recorded in two healthy pigs implanted with the rotary blood pump. Simulated responses of the model were shown to agree well with the experimental data over a range of pump operating points [6].

B. Implementation of deadbeat control algorithm

A deadbeat controller algorithm [10] was implemented to control the pump flow. The advantage of a deadbeat controller is in its ability to drive the system error to zero within a minimum possible sampling period [11]. The block diagram of the deadbeat control system was shown in Fig. 2. The input to the deadbeat controller is the reference pump flow, estimated differential pressure and estimated pump flow. The output of the controller is the pulse width modulation signal (PWM) to the rotary pump (u). Pump rotational speed (ω) and power (P) were the only variables measured in our system, and were used to estimate steady state pump flow, $f(.)$ [9]:

$$f = a_1 + a_2P + a_3P^2 + a_4P^3 + a_5\omega + a_6\omega^2 \qquad (1)$$

where $P = VI$ is the product of supply voltage (V) and motor current (I), and a_1-a_6 are functions of viscosity levels [12]. f was then used to estimate the pulsatile pump flow, Q_p, using the dynamical model derived in [9]:

$$\begin{aligned} Q_p(k\tau) &= 0.2710f([k-1]\tau) - 0.2546f([k-2]\tau) \\ &\quad -1.985Q_p([k-1]\tau) - 1.240Q_p([k-2]\tau) \\ &\quad -0.2397Q_p([k-3]\tau) + e_1(k\tau) \end{aligned} \qquad (2)$$

Here, τ is the sampling interval equal to 0.02s and $e_1(k\tau)$ represents the model error. The estimated pulsatile flow (Q_p), together with the rotational speed (ω), was then used to estimate the instantaneous differential pressure across the pump (H_p) [9], as defined by

$$\begin{aligned} H_p(k\tau) &= -0.476 - 1.157Q_p([k-1]\tau) \\ &\quad +1.519Q_p([k-2]\tau) - 0.278Q_p([k-3]\tau) \\ &\quad -0.475Q_p([k-4]\tau) + 0.0683\omega([k-1]\tau) \\ &\quad -0.0742\omega([k-2]\tau) - 0.0298\omega([k-3]\tau) \\ &\quad +0.0379\omega([k-4]\tau) - 1.735H_p([k-1]\tau) \\ &\quad +0.758H_p([k-2]\tau) + e_2(k\tau) \end{aligned} \qquad (3)$$

where $e_2(k\tau)$ represents the model error.

A new autoregressive with exogenous inputs (ARX) model with three input signals which describes the relationship between the control input signal, i.e. the PWM signal, u, the steady state pump flow, f, the pulsatile pump flow, Q_p, and the pump differential pressure, H_p were developed in the present study in order to design the control algorithm:

$$\begin{aligned} f(k\tau) &= d_1u([k-3]\tau) + d_2f([k-1]\tau) \\ &\quad -d_3f([k-2]\tau) + d_4Q_p([k-3]\tau) \\ &\quad +d_5H_p([k-3]\tau) + e_3(k\tau) \end{aligned} \qquad (4)$$

Here, d_1, d_2, d_3, d_4, d_5 are constants with values of 0.004199, 1.956, -0.962, 0.05766, and -0.0005538 respectively and $e_3(k\tau)$ represents the model error. Order and parameters of the ARX model which produced the smallest mean absolute error (e) between the estimated and the measured f were chosen, based on data obtained from the mock loop experiments described in [9].

In the present simulation, two cases were simulated: (i) constant reference input, i.e. $r(t) = a$, where a = constant > 0, and (ii) sinusoidal reference input, i.e. $r(t) = a + b\sin(\omega t)$, where $a\&b$ = constant, $a > b$. In order to achieve the reference value, r, we derived our control input, u, based on (4):

$$\begin{aligned} u(k\tau) &= \frac{1}{d_1}(\overline{f}([k+3]\tau) - d_2 f([k+2]\tau) \\ &\quad + d_3 f([k+1]\tau) - d_4 Q_p(k\tau) \\ &\quad - d_5 H_p(k\tau)) \end{aligned} \tag{5}$$

where $\overline{f}$ is the desired steady state pump flow, which was derived based on (2):

$$\begin{aligned} \overline{f}(k\tau) &= \frac{1}{0.271}(0.2397 Q_p([k-2]\tau) + 1.240 Q_p([k-1]\tau) \\ &\quad + 1.985 Q_p(k\tau) + 0.2546 f([k-1]\tau) \\ &\quad + r([k+1]\tau)) \end{aligned} \tag{6}$$

To represent model uncertainty, a sinusoidal high frequency signal at 20 Hz were added to the model error terms, e_1-e_3 in Eqs. (2), (3) and (4).

III. RESULTS AND DISCUSSION

There is a high correlation between our measured and simulated steady state pump flow (f), with an R^2 value of 0.945 (slope of linear regression line = 0.961).

The simulation was first carried out using varying levels of reference pump flow input to study the hemodynamic response of the CVS under various heart conditions, i.e. (i) healthy, (ii) moderate LVF and (iii) severe LVF. Fig. 3 shows the effect of mean pump flow on cardiac output (CO), mean aortic valve flow (mQ_{av}), mean aortic pressure (mP_{ao}) and mean left atrial pressure (mP_{la}). With increasing degree of LVF, cardiac output and mean arterial pressure decreases while left atrial pressure increases. As observed experimentally, total cardiac output and mean arterial pressure increases the most in severe LVF patients, followed by, followed by moderate LVF patients and healthy subjects [13]. On the other hand, increasing pump flow decreases left atrial pressure in all three cases of varying heart conditions, leading to a decrease in stroke volume and aortic valve flow through the Frank-Starling mechanism. This is consistent with published findings [14], [15].

Next, sinusoidal signals of varying mean values, amplitudes and phase shifts (as defined in Fig. 4) were applied to the reference pump flow input. In all simulations, frequencies of the sinusoidal signals were chosen to be equal to the heart rates.

Fig. 5 shows the waveforms of the aortic pressure (P_{ao}), aortic valve flow (Q_{av}) and pump flow (Q_p) superimposed on the reference pump flow signal (r) generated by the model using parameters for the severe LVF condition. The reference input signal was increased from $r(t)$=2.5+1.5sin(ωt) to $r(t)$=5+1.5sin(ωt) at t=10s. It is shown that the simulated pump flow accurately tracked the reference input signal within an error of $\pm$0.7 L/min.

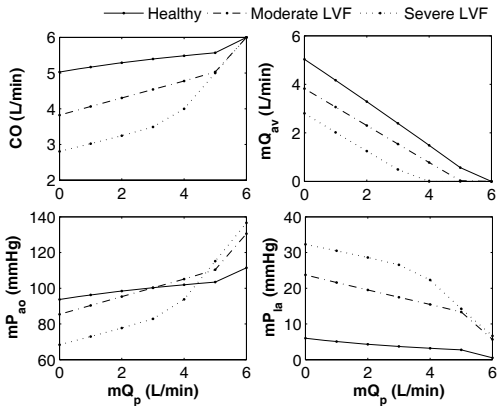

Fig. 3. Effect of mean pump flow (mQ_p) on total cardiac output (CO), mean aortic valve flow (mQ_{av}), mean aortic pressure (mP_{ao}) and mean left atrial pressure (mP_{la}) under three different heart conditions: healthy, moderate and severe LVF.

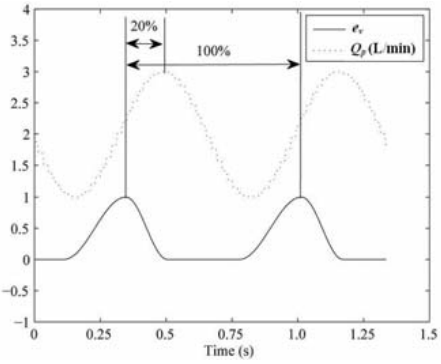

Fig. 4. Definition of phase shift in the present study: phase shift for the sinusoidal reference pump flow input, Q_p, is defined as 0 when the peak pump flow value occurs during end systole, i.e. at the maximum value of the time varying elastance function, ev.

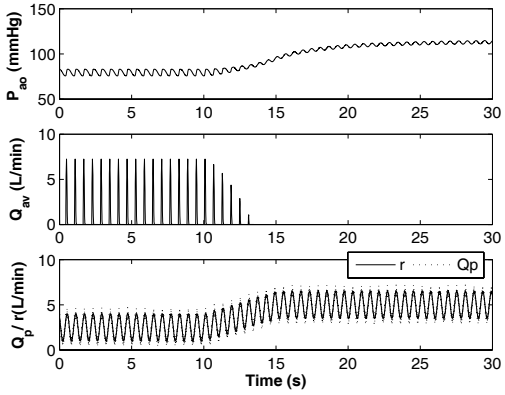

Fig. 5. Aortic pressure (Pao), aortic valve flow (Qav), pump flow (Qp) and reference pump flow (r) waveforms from the model simulations using parameters for severe LVF condition. Reference pump flow input was increased linearly from $2.5 + 1.5sin(\omega t)$ L/min at $t = 10s$ to $5 + 1.5sin(\omega t)$ L/min at $t = 15s$.

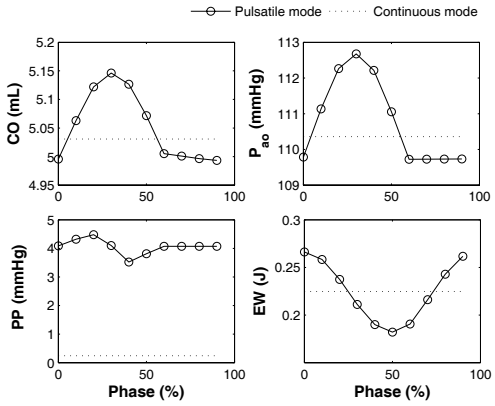

Fig. 6. Effect of sinusoidal pump flow modulation on mean cardiac output (CO), mean arterial pressure (mP_{ao}), pulse pressure (PP) and external work (EW) at different phase shifts.

Fig. 6 showed the effect of sinusoidal pump flow modulation on mean cardiac output (CO), mean arterial pressure (mP_{ao}), pulse pressure (PP) and external work (EW) at different phase shifts, using parameters for the moderate LVF subject. Mean cardiac output and mean arterial pressure were not affected by sinusoidal pump flow modulation but pulse pressure was increased. In terms of left ventricular external stroke work, counterpulsation (50% phase shift) produced the minimum stroke work, as observed by Vandenberghe et al. [16], which is helpful for left ventricular recovery.

IV. CONCLUSIONS

In this paper, we examined the performance of a deadbeat controller in the presence of model uncertainty under both continuous and pulsatile model conditions, with varying degrees of heart failure. Results showed that the controller is able to track the reference input with minimal error, by using noninvasive measurements. Counterpulsation mode is most beneficial for myocardial recovery as it decreases left ventricular external work and oxygen consumption.

REFERENCES

[1] Y. Wu, P. Allaire, G. Tao, and D. Olsen, "Study of pressure estimation for a human circulatory system with a lvad," in *Proceedings of the 2006 American Control Conference*, 2006, pp. 713–718.

[2] S. Choi, J. F. Antaki, J. R. Boston, and D. Thomas, "A sensorless approach to control of a turbodynamic left ventricular assist system," *IEEE Transactions on Control System Technology*, vol. 9, no. 3, pp. 473–482, 2001.

[3] M. Thalmann, H. Schima, G. Wiselthaler, and E. Wolner, "Physiology of continuous blood flow in recipients of rotary cardiac assist devices," *Journal of Heart and Lung Transplantation*, vol. 24, pp. 237–245, 2005.

[4] T. Korakianitis and Y. Shi, "Numerical comparison of hemodynamics with atrium to aorta and ventricular apex to aorta vad support," *ASAIO Journal*, vol. 53, pp. 537–548, 2007.

[5] S. Vandenberghe, P. Segers, J. Antaki, B. Meyns, and V. PR, "Hemodynamic modes of ventricular assist with a rotary blood pump: continuous, pulsatile, and failure," *ASAIO Journal*, vol. 51, pp. 711–718, 2005.

[6] E. Lim, S. Dokos, S. Cloherty, R. F. Salamonsen, D. G. Mason, and N. H. Lovell, "Parameter-optimized model of cardiovascular-rotary blood pump interactions," *submitted to IEEE Transactions on Biomedical Engineering, 2009*.

[7] A. C. Guyton and J. E. Hall, *Textbook of Medical Physiology*. Philadelphia, Pennsylvania: W. B. Saunders Company, 1996.

[8] S. E. Epstein, G. D. Beiser, M. Stampfer, B. F. Robinson, and E. Braunwald, "Characterization of the circulatory response to maximal upright exercise in normal subjects and patients with heart disease," *Circulation*, vol. 35, pp. 1049–62, 1967.

[9] A. AlOmari, A. Savkin, D. Karantonis, E. Lim, and L. NH, "Non-invasive estimation of pulsatile flow and differential pressure in an implantable rotary blood pump for heart failure patients," *Physiological Measurement*, vol. 30, pp. 371–386, 2009.

[10] K. Astrom and B. Wittenmark, *Computer Controlled Systems (3rd ed.)*. Longman Higher Education, 1997.

[11] K. Ogata, *Discrete-Time Control Systems (2nd ed)*. Englewood Cliffs, NJ: Prentice Hall, 1994.

[12] N. Malagutti, D. M. Karantonis, S. L. Cloherty, P. J. Ayre, D. G. Mason, R. F. Salamonsen, and N. H. Lovell, "Non-invasive average flow estimation for an implantable rotary blood pump: a new algorithm incorporating the role of blood viscosity," *Artificial Organs*, vol. 31, pp. 45–52, 2007.

[13] B. Meyns, T. Siess, Y. Nishimura, R. Racz, H. Reul, G. Rau, V. Leunens, and W. Flameng, "Miniaturized implantable rotary blood pump in atrial-aortic position supports and unloads the failing heart," *Cardiovascular Surgery*, vol. 6, no. 3, pp. 288–95, 1998.

[14] A. H. Goldstein, G. Monreal, A. Kambara, A. J. Spiwak, M. L. Schlossberg, A. R. ABrishamchian, and M. A. Gerhardt, "Partial support with a centrifugal left ventricular assist device reduces myocardial oxygen consumption in chronic, ischemia heart failure," *Journal of Cardiac Failure*, vol. 11, no. 2, pp. 142–151, 2005.

[15] S. Kono, K. Nishimura, T. Nishina, S. Yuasa, K. Ueyama, C. Hamada, T. Akamatsu, and M. Komeda, "Autosynchronized systolic unloading during left ventricular assist with a centrifugal pump," *Journal of Thoracic & Cardiovascular Surgery*, vol. 125, no. 2, pp. 353–60, 2003.

[16] S. Vandenberghe, P. Segers, B. Meyns, and P. Verdonck, "Unloading effect of a rotary blood pump assessed by mathematical modeling," *Artificial Organs*, vol. 27, no. 12, pp. 1094–101, 2003.